

Geometry-aware Temporal Aggregation Network for Monocular 3D Lane Detection

Huan Zheng*, Wencheng Han*, Tianyi Yan, Cheng-zhong Xu, Jianbing Shen[†]
SKL-IOTSC, CIS, University of Macau

Abstract

Monocular 3D lane detection aims to estimate 3D position of lanes from frontal-view (FV) images. However, current monocular 3D lane detection methods suffer from two limitations, including inaccurate geometric information of the predicted 3D lanes and difficulties in maintaining lane integrity. To address these issues, we seek to fully exploit the potential of multiple input frames. First, we aim at enhancing the ability to perceive the geometry of scenes by leveraging temporal geometric consistency. Second, we strive to improve the integrity of lanes by revealing more instance information from temporal sequences. Therefore, we propose a novel Geometry-aware Temporal Aggregation Network (GTA-Net) for monocular 3D lane detection. On one hand, we develop the Temporal Geometry Enhancement Module (TGEM), which exploits geometric consistency across successive frames, facilitating effective geometry perception. On the other hand, we present the Temporal Instance-aware Query Generation (TIQG), which strategically incorporates temporal cues into query generation, thereby enabling the exploration of comprehensive instance information. Experiments demonstrate that our GTA-Net achieves SoTA results, surpassing existing monocular 3D lane detection solutions.

1. Introduction

3D lane detection stands as a cornerstone within the realm of autonomous driving systems. Its primary objective involves the meticulous estimation of lane line 3D coordinates [36]. Accurate perception of 3D lanes across diverse environments is crucial, not only for ensuring adherence to lane boundaries and consistent lane keeping [46], but also for enabling important downstream tasks such as high-definition map construction [23, 27, 32] and trajectory planning [1, 50]. Considering the cost-effectiveness of sensors and the rich color information provided by visual data, monocular vision-based 3D lane detection has become

*Equal contribution. [†]Corresponding author: Jianbing Shen.

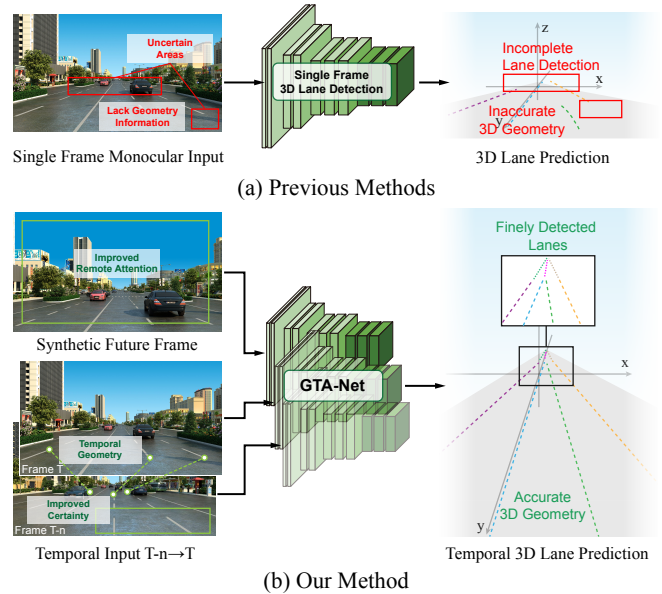


Figure 1. **Comparison with Monocular 3D Lane Detection Approaches.** (a) Existing methods [2, 5, 10, 13, 17] that rely on a single frame as input are hindered by inaccuracies in 3D geometry perception and difficulties in maintaining lane integrity. (b) In contrast, our approach, which incorporates multiple frames along with synthetic future frames, facilitates improved 3D geometric perception and enables integral lane detection within the scene.

a pivotal research direction in autonomous driving [36].

Estimating lanes in 3D space from a 2D image is a formidable challenge, primarily due to the lack of depth cues. To address this, some methods decompose 3D lane detection into two stages: first detecting lanes in 2D, then projecting them into 3D space [54]. Specifically, SALAD [54] tackles this problem by performing two tasks: 2D lane segmentation and dense depth estimation, which together facilitate 3D lane detection. After segmenting the 2D lanes, they are projected into 3D space using camera intrinsics and the predicted depth information. However, this approach still faces two significant drawbacks: it relies heavily on the accuracy of depth estimation and demonstrates suboptimal performance in 3D lane detection.

An alternative approach involves detecting lanes from

a bird’s-eye-view (BEV) perspective [5, 10, 13, 31, 48]. These BEV-based methods decompose 3D lane detection into two tasks: 2D lane detection in BEV space and corresponding height estimation. Typically, they employ inverse perspective mapping (IPM) [37] to warp image features from the frontal-view (FV) space to BEV, effectively transforming perspective-view (PV) features into BEV features. To project the detected BEV lanes into 3D space, the BEV coordinates are combined with the corresponding height values which serve as representations of the 3D lanes. However, these BEV-based methods still suffer from the following limitations. Firstly, IPM operates under the assumption of a level surface, making it less effective in scenarios involving uphill or downhill slopes where the road surface deviates from flat terrain. Secondly, due to its reliance on ground-based image warping, IPM inevitably sacrifices valuable height details and contextual information above the road surface. Thirdly, BEV features, unlike perspective features, lack the ability to perceive distant information, thus exhibiting a more limited perception range.

To tackle the aforementioned challenges, recent methodologies incorporate 3D anchors or queries to sample FV features in the context of monocular 3D lane detection [2, 3, 17, 35]. These 3D anchors or queries serve as pivotal elements, used to generate 2D coordinates in image coordinates to sample relevant features. Subsequently, cross-attention mechanisms are employed, allowing for information interaction and iterative refinement of these anchors or queries. This integration is capable of providing a more comprehensive understanding of the spatial context, ultimately leading to improved performance for monocular 3D lane detection in challenging scenarios.

However, current monocular 3D lane detection methods are constrained by two limitations, including *the inaccurate geometric representation of predicted 3D lanes and the difficulty in maintaining lane integrity*. These challenges may lead to suboptimal performance in real-world applications. As shown in figure 1 (a), the predicted results exhibit the following issues: errors in the positioning of the lanes within 3D space, and incomplete detection, with some lanes being only partially identified or even missed entirely. In this paper, we aim to address these limitations by fully leveraging the potential of multiple input frames from two complementary perspectives, as expressed in figure 1 (b). Firstly, we focus on enhancing the ability to perceive the geometry of scenes by exploiting temporal geometric consistency across consecutive frames. This allows for more accurate and stable estimations of lane positions in 3D space. Secondly, we seek to improve the integrity of lanes by leveraging temporal sequences to extract comprehensive lane instance information. In detail, we leverage images from historical frames and a synthesized future frame to capture instance information for both near and dis-

tant regions, thereby mitigating uncertainties in these areas to improve lane integrity.

Based on the aforementioned insight, we propose an end-to-end monocular 3D lane detection framework, named Geometry-aware Temporal Aggregation Network (GTA-Net). To be specific, we introduce two novel modules in our work including Temporal Geometry Enhancement Module (TGEM) and Temporal Instance-aware Query Generation (TIQG). TGEM effectively leverages geometric consistency across consecutive frames, enabling accurate geometric perception of the scene. Meanwhile, TIQG strategically incorporates temporal cues into query generation, facilitating the comprehensive utilization of temporal instance information to enhance lane integrity. These generated queries from TIQG, along with the geometry-aware features from TGEM, are then fed into a deformable attention-based decoder, facilitating iterative information interaction. Finally, a Multilayer Perceptron (MLP)-based 3D lane detection head is employed to produce the final 3D lane predictions.

In brief, the paper presents the following contributions:

- We propose the Geometry-aware Temporal Aggregation Network (GTA-Net) for monocular 3D lane detection, which achieves highly reliable predictions by effectively leveraging temporal information.
- We introduce the Temporal Geometry Enhancement Module (TGEM) to enhance the geometric perception of the scene by exploiting the geometric consistency between consecutive frames.
- We develop the Temporal Instance-aware Query Generation (TIQG) to generate lane queries by fully utilizing the potential of instance information in temporal cues to alleviate difficulties in maintaining lane integrity.
- Experimental results show that the proposed GTA-Net outperforms existing monocular 3D lane detection methods, achieving state-of-the-art performance.

2. Related Work

2.1. 2D Lane Detection

2D lane detection, a critical aspect of autonomous driving, strives to precisely determine the shapes and positions of lanes within images [45, 53]. With the development of deep learning [4, 8, 21, 51], deep neural network-based 2D lane detection has achieved remarkable strides forward [14, 20, 40, 47, 59]. According to the formulation of 2D lane detection, existing solutions can be divided into four categories: segmentation-based, anchor-based, keypoint-based and curve-based methods [17].

Segmentation-based approaches [22, 24, 58] employ segmentation tasks as intermediaries for executing lane detection. To be specific, these methods firstly complete pixel-wise classification to obtain 2D lane segmentation masks. Next, the segmentation masks are processed by

some carefully-design strategies to construct a set of lanes. Anchor-based approaches primarily utilize line-like anchors for regressing offsets relative to ground truth lanes [19, 29, 39, 40, 43, 56]. To enhance the efficacy of line-shape anchors, row-based anchors have been devised for capitalizing on the natural shape of lanes [56]. By using row-based anchors, 2D lane detection task is converted into a row-wise classification problem. Furthermore, these row-based and column-based anchors are combined to reduce the occurrence of localization errors in side lanes [40]. Keypoint-based approaches offer a flexible framework for modeling lane positions [22, 41, 47]. At the outset, these methodologies embark on predicting the 2D coordinates of pivotal points along the lanes [22]. Following this initial step, a diverse array of strategies is employed to effectively group these key points into distinct lanes [47]. Curve-based approaches leverage a range of curve formulations to model lanes [9, 30, 44]. Specifically, this type of method aims to estimate the parameters of curves to obtain 2D lane detection results. BézierLaneNet [9] leverages the parametric Bézier curve for its computational simplicity, stability, and extensive flexibility in transformations. Additionally, the authors introduce a novel feature flip fusion module, which takes into account the symmetrical characteristics of lanes within driving environments.

2.2. 3D Lane Detection

The objective of 3D lane detection is to identify lanes within 3D space and accurately estimate their coordinates [25, 36, 60]. In contrast to 2D lane detection, 3D lane detection methods need to perceive the geometric information of scenes. Some methodologies try to enhance perception accuracy by leveraging both lidar and camera data [33, 34]. However, the acquisition and annotation expenses associated with multi-modal data are prohibitively high, constraining the practical implementation of such methodologies. Hence, monocular 3D lane detection garners increased interest due to its provision of a cost-effective alternative to multi-modal methodologies [36].

Monocular 3D lane detection is challenging due to the absence of depth information. To address this issue, SALAD [54] incorporates a depth prediction branch to estimate depth, which is used to project 2D lanes to 3D space. However, employing depth estimation in the process of detecting lanes may introduce cumulative errors and further exhibits inferior performance. IPM-based approaches have become increasingly prominent owing to their advantageous geometric properties for lane depiction in BEV perspective [36]. 3D-LaneNet [10] utilizes IPM for the conversion of FV features into BEV features, enabling bidirectional information flow between image-view and top-view representations. Next, these features are leveraged for learning the anchor offsets of lanes in the BEV space. Gen-

LaneNet [13] introduces a novel lane anchor representation guided by geometry in a newly defined coordinate system, which employs a specific geometric transformation to directly compute real 3D lane points from the network output. It is essential to emphasize that aligning the lane points with the underlying top-view features in the newly defined coordinate frame is crucial for establishing a generalized method capable of effectively handling diverse scenes.

IPM relies heavily on the ground plane assumption, which cannot be guaranteed in real scenarios [6]. To solve this issue, Anchor3DLane [17] is introduced, eliminating the need for BEV representation and instead utilizing 3D lane anchors directly in 3D space. These 3D lane anchors are projected onto image coordinate system for feature extraction, capturing both structural and contextual information crucial for precise lane detection. LATR [35] uses a transformer-based architecture for monocular 3D lane detection. Specifically, the authors design a lane-aware query generator that produces queries derived from 2D lane segmentation. Besides, dynamic 3D ground PE generator is presented to embed 3D information during query update.

3. Method

In this section, we will initially present a comprehensive introduction to the proposed Geometry-aware Temporal Aggregation Network (GTA-Net) in Section 3.1. To enhance the understanding of the geometric structure inherent in driving scenes, we introduce Temporal Geometry Enhancement Module (TGEM) in Section 3.2. Following this, we introduce Temporal Instance-aware Query Generation (TIQG) aimed at generating queries by fully utilizing temporal information in Section 3.3. Finally, we delve into the employed loss functions in Section 3.4.

3.1. Overall Architecture

Given successive front-view images I_t and $I_{t-n} \in \mathbb{R}^{3 \times H \times W}$, the objective of monocular 3D lane detection is to estimate the 3D coordinates of the lane lines in the image I_t . Each 3D lane can be described by a set of 3D points along with the corresponding lane category:

$$L = (P, C), \quad P = (x_i, y_i, z_i)_{i=1}^N, \quad (1)$$

where L denotes a 3D lane, C represents the corresponding lane category of L , P is composed of N 3D points with N being a predefined parameter. It is noted that the sequence $\{y_1, y^2, \dots, y^N\}$ is often defined as a predetermined longitudinal coordinate [5, 10, 13]. Based on the above descriptions about lane representation, the 3D lanes in an input image I_t can be represented as $G = \{L^1, L^2, \dots, L^M\}$, where G represent the collection of all 3D lanes, and M denotes the number of 3D lanes.

The overall architecture of our GTA-Net is illustrated in figure 2. Initially, a 2D backbone network is utilized to ex-

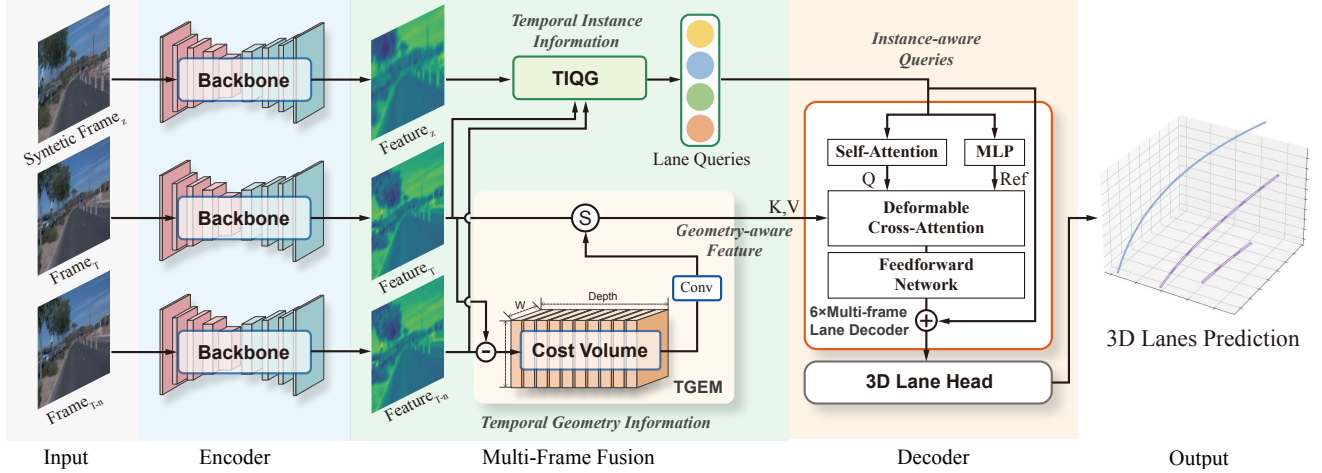


Figure 2. **Illustration of the Overall Architecture of the Proposed GTA-Net.** The input images are first fed into a backbone network to extract 2D perspective features. Next, TGEM is applied to enhance the geometric perception of the scene. Simultaneously, TIQG is used to generate lane queries. These lane queries and features are sent to the lane decoder to obtain the final 3D lane predictions.

tract image features F_t and F_{t-n} from the input front-view images I_t and I_{t-n} :

$$F_t = \text{Backbone}(I_t), \quad F_{t-n} = \text{Backbone}(I_{t-n}), \quad (2)$$

where $\text{Backbone}(\cdot)$ denotes transformation of the used 2D backbone network. Subsequently, the Temporal Geometry Enhancement Module (TGEM) takes these image features F_t and F_{t-n} as input to obtain geometry-aware features:

$$F_{ge} = \text{TGEM}(F_{t-n}, F_t), \quad (3)$$

where F_{ge} and $\text{TGEM}(\cdot)$ indicate geometry-aware features and the transformation of TGEM, respectively. TGEM aims to learn the geometric relationships between successive frames, thereby enhancing the depth perception capability of our GTA-Net in driving scenes. Simultaneously, image features F_t and F_{t-n} are sent to Temporal Instance-aware Query Generation (TIQG), which generates queries by making full use of temporal instance information. This process can be formulated as follows:

$$Q = \text{TIQG}(F_{t-n}, F_t), \quad (4)$$

where Q represents the generated instance-aware queries, and $\text{TIQG}(\cdot)$ denotes the transformation performed by the TIQG module. Next, the instance-aware queries Q and geometry-aware features F_{ge} are fed into a deformable attention [52, 61] based decoder to iteratively update queries:

$$Q_u = \text{Decoder}(Q, F_{ge}), \quad (5)$$

where Q_u and $\text{Decoder}(\cdot)$ denote the updated queries and the transformation of the above deformable attention-based decoder, respectively. Finally, the updated queries Q_u are

fed into the 3D lane detection head to output the predictions of 3D lanes in the input image I_t , which can be described as follows:

$$\hat{G} = \text{Head}(Q_u), \quad (6)$$

where \hat{G} indicates the estimated 3D lanes, and $\text{Head}(\cdot)$ denotes 3D lane detection head.

3.2. Temporal Geometry Enhancement Module

The inherent absence of depth cues in monocular input images poses a significant challenge for monocular 3D lane detection solutions. Without depth information, accurately understanding the complex geometric details of driving scenes becomes difficult. Drawing inspiration from prior research [49, 55] in monocular depth estimation, this study aims to alleviate this limitation by utilizing the geometric relationship between consecutive frames. To this end, we propose Temporal Geometry Enhancement Module (TGEM), which is designed to delve into the geometric consistency hidden in successive frames. The structure of TGEM is described by figure 2. In detail, TGEM consists of three main stages: cost volume construction, geometric feature learning and geometry-aware feature enhancement.

Cost volume construction. To uncover the potential geometric information within successive monocular images, we first construct a cost volume in the initial stage of TGEM. This is because the cost volume is capable of capturing the geometric relationship between adjacent frames [11].

Starting with 2D features F_t and F_{t-n} extracted from the 2D backbone network, we replicate these features D times along the depth dimension, where D represents a designated depth range. The process can be formulated as follows:

$$E_t = \text{Repeat}(F_t), \quad E_{t-n} = \text{Repeat}(F_{t-n}), \quad (7)$$

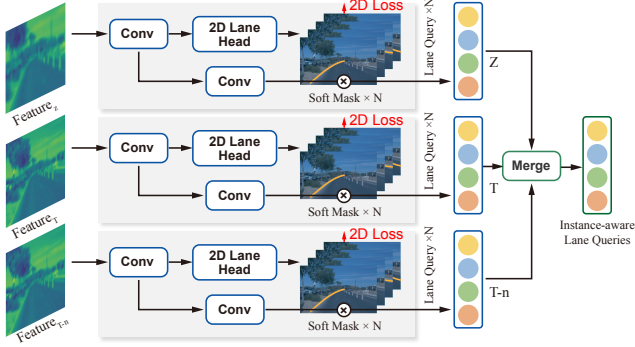


Figure 3. **An Overview of the Proposed Temporal Instance-aware Query Generation (TIQG) Module.** TIQG strategically integrates temporal cues into the query generation process, thereby enhancing its capacity to exploit temporal instance information for the promotion of lane integrity.

where E_t and E_{t-n} denote the expanded features, and $\text{Repeat}(\cdot)$ represents the feature expanding operation. Next, the expanded features E_{t-n} in image coordinate system of $t-n$ frame is projected onto image coordinate system of t frame by using camera intrinsics, extrinsics and lidar poses:

$$\hat{E}_t = \text{Warp}(E_{t-n}), \quad (8)$$

where \hat{E}_t denotes the warped features in image coordinate system of t frame, and $\text{Warp}(\cdot)$ indicates the projection from image coordinate system of $t-n$ frame to image coordinate system of t frame. In the final step, the matching cost between \hat{E}_t and E_t is computed by using l_1 norm:

$$C = \|\hat{E}_t - E_t\|_1, \quad (9)$$

where $\|\cdot\|_1$ denotes the transformation of l_1 norm, and C indicates the cost volume between the input successive front-view images I_t and I_{t-n} .

Geometric feature learning. Once the cost volume between successive front-view images is obtained, we utilize cascaded 2D convolution, batch normalization layer, and ReLU activation function to transform the cost volume into geometric features. This transformation can be expressed as follows:

$$F_g = \text{ReLU}(\text{BN}(\text{Conv}(C))), \quad (10)$$

where F_g denotes geometric features containing the 3D structural information of the driving scene, and $\text{Conv}(\cdot)$, $\text{BN}(\cdot)$ and $\text{ReLU}(\cdot)$ represent the transformation of 2D convolution, batch normalization layer and ReLU activation function, respectively.

Geometry-aware feature enhancement. To enrich the geometric perception capability of our GTA-Net, we aim to dynamically infuse geometric features into 2D features of t frame. To be specific, we first utilize geometric features F_g to derive two learnable tensors: weights α and residual β :

$$\alpha = \text{Sigmoid}(\text{BN}(\text{Conv}(F_g))), \quad (11)$$

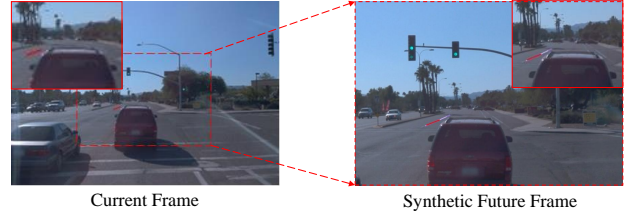


Figure 4. **Monocular Lane Detection Results of Setting Current and the Synthetic Future Frames as Input.** The white line represents the predicted lane line and the red line denotes the gt. We see that the lane line is missing in the predictions when accepting the current frame. In contrast, there is a white line in the visual results for treating the synthetic future frame as input.

$$\beta = \text{ReLU}(\text{BN}(\text{Conv}(F_g))), \quad (12)$$

where $\text{Sigmoid}(\cdot)$ denotes the transformation of sigmoid activation function. Subsequently, the weights α and residual β are used to inject geometric information into 2D features:

$$F_{ge} = \alpha F_t + \beta. \quad (13)$$

As a result, the feature enhancement mechanism enables our GTA-Net to dynamically adjust and integrate geometric information into the feature extraction process, thereby enhancing its ability to perceive intricate geometric structures within the scene.

3.3. Temporal Instance-aware Query Generation

Successive frames provide different perspectives of the driving scene. Each frame contains unique contextual cues and dynamic changes within the scene. In addition to the geometric consistency between successive frames, we also aim to leverage the information variety between them, revealing rich instance information to alleviate the difficulties in maintaining lane integrity. Hence, we propose the Temporal Instance-aware Query Generation (TIQG), as shown in figure 3. There are three main steps in TIQG including initial query generation, synthetic future query generation and temporal query aggregation.

Initial query generation. The initial query generation process involves generating temporal queries for both frame t and frame $t-n$. The queries consist of two-level embeddings: instance-level embeddings and point-level embeddings. To derive instance-level embedding, cascaded 2D convolutions are employed to process image features F_t and F_{t-n} as follows:

$$Q_t^l = \text{Conv}(F_t), \quad Q_{t-n}^l = \text{Conv}(F_{t-n}), \quad (14)$$

where Q_t^l and Q_{t-n}^l denote the generated instance-level embeddings of frame t and frame $t-n$, respectively. For point-level embedding, we define two learnable parameters Q_t^p and Q_{t-n}^p . Subsequently, these corresponding two-level embeddings are merged using the following formulation:

$$Q_t = Q_t^l \oplus Q_t^p, \quad Q_{t-n} = Q_{t-n}^l \oplus Q_{t-n}^p, \quad (15)$$

Table 1. **Quantitative Comparison of Monocular 3D Lane Detection Solutions on the OpenLane Dataset.** ↓ and ↑ indicate that lower and higher values, respectively, signify superior performance. **Bold** numbers represent the best results, while underlined numbers indicate the second best. GTA-Net obtains the competitive performance on F1-score, lane category accuracy, x/z errors for both near and far range.

Methods	F1 (%) ↑	Category Accuracy (%) ↑	X error (m) ↓		Z error (m) ↓	
			<i>near</i>	<i>far</i>	<i>near</i>	<i>far</i>
3DLaneNet [10]	44.1	-	0.479	0.572	0.367	0.443
GenLaneNet [13]	32.3	-	0.593	0.494	0.140	0.195
Cond-IPM	36.6	-	0.563	1.080	0.421	0.892
Persformer [5]	50.5	89.5	0.319	0.325	0.112	0.141
CurveFormer [2]	50.5	-	0.340	0.772	0.207	0.651
BEV-LaneDet [48]	58.4	-	0.309	0.659	0.244	0.631
Anchor3DLane [17]	53.1	90.0	0.300	0.311	0.103	0.139
DecoupleLane [15]	51.2	-	-	-	-	-
CurveFormer++ [3]	52.5	87.8	0.333	0.805	0.186	0.687
LaneCMK [57]	55.8	89.2	0.310	0.303	0.083	0.123
GroupLane [26]	60.2	91.6	0.371	0.476	0.220	0.357
CaliFree3DLane [12]	56.4	-	0.319	0.767	0.245	0.706
CaliFree3DLane* [12]	57.0	-	0.306	0.761	0.227	0.683
3DLaneFormer [7]	55.0	89.9	0.283	0.305	0.106	0.138
Ours	62.4	92.8	0.225	0.254	0.078	0.110

where \oplus represents the broadcasting summation.

Synthetic future query generation. As shown in figure 4, the 3D lane is not detected at the intersection, likely due to increased distance of the lane from the camera. To mitigate this issue, we seek to reduce the distance between the camera and the lane. A straightforward approach would involve using a future frame; however, real-world applications do not provide access to future information. As a solution, we synthesize a future frame by zooming in on the scene. This synthetic frame is then fed into the 3D lane detection model. Notably, we observe that lanes, which were initially undetected, become discernible in the synthetic future frame. This observation motivates the generation of pseudo-future frame to effectively detect lanes distant regions.

Based on the aforementioned analysis, we design the synthetic future query generation. Initially, we first crop and magnify the input image I_t to generate a synthetic future frame. Then, this synthetic future frame undergoes feature extraction to derive 2D perspective features F_p . Once the 2D perspective features F_p are obtained, the corresponding queries can be formulated as follows:

$$Q_p^l = \text{Conv}(F_p), \quad Q_p = Q_p^l \oplus Q_p^p, \quad (16)$$

where Q_p denotes synthetic future queries, while Q_p^l and Q_p^p are instance-level embedding and point-level embedding, respectively. By integrating both instance-level and point-level embeddings, TIQG gains a comprehensive understanding of the distant context, enhancing its capability to detect 3D lanes in distant regions.

Temporal query aggregation. To fully explore temporal context, the information in these temporal queries Q_t , Q_{t-1} and Q_p are interacted by using cross-attention in the step of

temporal query aggregation, which can be described by:

$$Q_p^u = \text{CA}(Q_p, Q_t), \quad Q_{t-1}^u = \text{CA}(Q_{t-1}, Q_t), \quad (17)$$

where Q_p^u , Q_{t-1}^u and $\text{CA}(\cdot)$ denote the updated synthetic future queries, the updated queries of frame $t - 1$ and the transformation of cross-attention. Subsequently, these lane queries are fed into cascaded convolutions to obtain instance-aware queries Q :

$$Q = \text{Conv}(\text{Concat}(Q_t, Q_{t-1}, Q_p)), \quad (18)$$

where $\text{Concat}(\cdot)$ denotes concatenation operation. The instance-aware queries integrate rich instance-aware information, thereby enhancing the capacity to comprehensively perceive lanes to promote lane integrity.

3.4. Loss Function

With the matched ground truth 3D lanes corresponding to the output 3D lane queries, we compute the loss for each respective pair. To be specific, L1 loss is employed to regress the x -coordinates and z -coordinates. Binary cross-entropy loss is used to enforce the visibility constraint of the output 3D lanes. Focal loss [28] is utilized to optimize the predicted lane category. In addition, a 2D segmentation loss is also included as an auxiliary loss. Hence, the final objective function of our GTA-Net can be formulated as follows:

$$\begin{aligned} \mathcal{L}_{total} = & \mathcal{L}_{vis} + w_x \mathcal{L}_x + w_z \mathcal{L}_z \\ & + w_{cate} \mathcal{L}_{cate} + w_{seg} \mathcal{L}_{seg}. \end{aligned} \quad (19)$$

where \mathcal{L}_{total} denotes the total loss, w_x , w_z , w_{cate} and w_{seg} are hyperparameters.

Table 2. **Quantitative Comparison of Monocular 3D Lane Detection Methods on the OpenLane Dataset Under Different Scenarios.** **Bold** numbers denote the best results. "All" indicates the average value of F1 scores in all scenarios. The proposed GTA-Net achieves superior performance under various extremely challenging scenarios than other solutions.

Methods	All	Up & Down	Curve	Extreme Weather	Night	Intersection	Merge & Split
3DLaneNet [10]	44.1	40.8	46.5	47.5	41.5	32.1	41.7
GenLaneNet [13]	32.3	25.4	33.5	28.1	18.7	21.4	31.0
PersFormer [5]	50.5	42.4	55.6	48.6	46.6	40.0	50.7
CurveFormer [2]	50.5	45.2	56.6	49.7	49.1	42.9	45.4
BEV-LaneDet [48]	58.4	48.7	63.1	53.4	53.4	50.3	53.7
Anchor3DLane [17]	54.3	47.2	58.0	52.7	48.7	45.8	51.7
DecoupleLane [15]	51.2	43.5	57.3	-	48.9	43.5	-
LATR [35]	61.9	55.2	68.2	57.1	55.4	52.3	61.5
CurveFormer++ [3]	52.7	48.3	59.4	50.6	48.4	45.0	48.1
LaneCMK [57]	55.8	47.3	58.6	53.2	48.0	42.2	51.7
CaliFree3DLane [12]	56.4	48.7	60.4	54.7	51.9	49.5	51.8
CaliFree3DLane* [12]	57.0	48.9	62.3	54.8	52.0	50.2	52.1
3DLaneFormer [7]	55.0	49.0	58.3	54.5	50.4	46.3	52.3
Anchor3DLane++ [18]	59.4	49.9	66.1	55.5	52.5	50.3	57.4
Ours	62.4	55.5	68.3	57.5	56.8	52.7	61.8

4. Experiments

This section provides a detailed overview of our experimental setup. We then evaluate the performance of our GTA-Net through a series of comparative analyses against state-of-the-art methods. Additionally, we present several ablation studies to gain a deeper understanding of the effectiveness of our proposed approach.

4.1. Experimental Setup

Dataset and Evaluation metrics. In the experiments, we use the OpenLane dataset [5], derived from the Waymo dataset [42], as a comprehensive benchmark for 3D lane detection. Comprising 1,000 segments and 200,000 frames, this dataset captures diverse environmental conditions such as varying weather, terrain, and lighting. The images in the OpenLane dataset have a resolution of 1280×1920 pixels and include 880,000 lane annotations spanning 14 categories. The OpenLane dataset provides a diverse and challenging set for evaluating 3D lane detection algorithms. We employ the official evaluation metrics to assess the effectiveness of our model on the OpenLane dataset. Specifically, we report the F1 score, lane category accuracy, and x/z errors in both the near and far ranges.

Implementation details. In our GTA-Net, we use ResNet-50 [16] as the 2D backbone network for extracting image features. Before feature extraction, all input images are resized to a resolution of 720×960. The experiments are conducted on the PyTorch platform using a workstation equipped with eight Tesla A100 GPUs, each with 40 GB of memory. For optimization, we employ the AdamW optimizer with a weight decay of 0.01. The initial learning rate

is set to $2e^{-4}$, and a cosine annealing scheduler is applied to gradually adjust the learning rate. Our model is trained for 24 epochs, with a batch size of 64. Additionally, we set $w_x = 2$, $w_z = 10$, $w_{cate} = 10$ and $w_{seg} = 5$.

Compared methods. We compare our GTA-Net with the following monocular 3D detection methods: 3DLaneNet [10], Gen-LaneNet [13], PersFormer [5], Cond-IPM, CurveFormer [2], DecoupleLane [15], Anchor3DLane [17], BEV-LaneDet [48], LATR [35], GroupLane [26], LaneCMK [57], CaliFree3DLane* [12], LaneCPP [38], 3DLaneFormer [7] and CurveFormer++ [3].

4.2. Main Results

Quantitative results. We present the experimental results of our method on the OpenLane dataset in Table 1. As shown in the results, our proposed GTA-Net outperforms existing state-of-the-art methods for 3D lane detection. Specifically, GTA-Net achieves the highest F1 score and lane category accuracy, underscoring its superior capability in accurately detecting 3D lanes while minimizing both missed detections and false positives. Moreover, when evaluating the localization of the detected 3D lanes, our method achieves competitive x/z errors under both far and near range in comparison to other monocular 3D lane detection approaches, further validating its effectiveness for perceiving both close and distant lanes.

To further validate the effectiveness of the proposed GTA-Net, we present results across a range of challenging scenarios. Table 2 reports the 3D lane detection performance on the OpenLane dataset under different conditions, measured by the F1 score. Notably, our method outper-

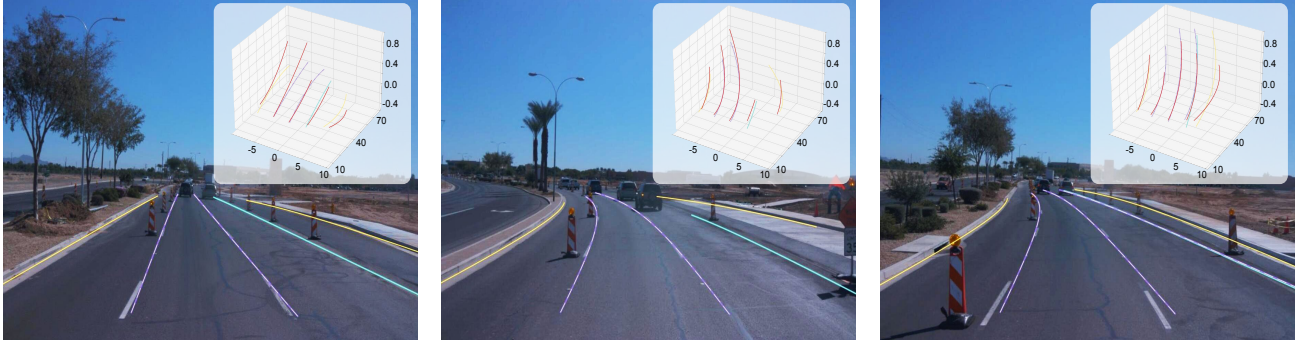


Figure 5. **Illustration of Predicted 3D Lanes on the OpenLane Dataset.** We present the predicted 3D lanes in both the perspective view and the 3D spatial representation. The red lines denote the ground truth lanes, while the other colored lines represent the predicted lanes.

Table 3. **Ablation Study of the Proposed Novel Modules Including TGEM and TIQG.** We have designed a series of variants to systematically evaluate the effectiveness of each individual module.

Methods	F1 (%) \uparrow	Category Accuracy (%) \uparrow	X error (m) \downarrow		Z error (m) \downarrow	
			<i>near</i>	<i>far</i>	<i>near</i>	<i>far</i>
<i>w/o.</i> TGEM	62.1	92.1	0.229	0.257	0.081	0.112
<i>w/o.</i> TIQG	62.1	91.7	0.229	0.264	0.080	0.114
Ours	62.4	92.8	0.225	0.254	0.078	0.110

forms existing approaches, achieving the highest F1 score across all scenarios. This demonstrates the robustness of our model in handling diverse driving environments, underscoring its reliability and efficacy in accurately detecting 3D lanes under varying real-world conditions.

Visual results. To rigorously assess the performance of GTA-Net, we present the visualization results on the OpenLane dataset. As depicted in figure 5, our model demonstrates the capability to accurately detect 3D lanes in the input images and to precisely estimate their corresponding positions in 3D space. These results illustrate the excellent performance of our model in accurately identifying and localizing lanes in 3D space.

4.3. Ablation Studies

We design a series of meticulous experiments to evaluate the efficacy of our approach in addressing the inherent challenges of monocular 3D lane detection. These experiments are carefully structured to provide a comprehensive understanding of how the proposed techniques contribute to improving overall performance.

Effect of TGEM. We first evaluate the contribution of the proposed TGEM module. As presented in Table 3, we assess the performance of GTA-Net without the TGEM module, denoted as *w/o* TGEM. The results demonstrate a marked degradation in performance, highlighting the critical role of TGEM in promoting the ability to capture and leverage geometric cues from the scene.

Effect of TIQG. We next evaluate the contribution of the TIQG module. As presented in Table 3, the variant labeled *w/o* TIQG corresponds to a version of GTA-Net where the TIQG module is omitted. The results reveal a significant degradation in performance across all metrics when TIQG is excluded, thereby suggesting its critical role in effectively leveraging temporal cues. This demonstrates the importance of TIQG in improving the accuracy of 3D lane detection from monocular inputs by harnessing temporal instance information to enhance the integrity of lanes.

5. Conclusion

In this paper, we tackle two key challenges in monocular 3D lane detection: the inaccurate geometric information of predicted 3D lanes and the difficulty in detecting remote lanes. To address these issues, we propose a novel Geometry-aware Temporal Aggregation Network (GTA-Net) for monocular 3D lane detection. We introduce the Temporal Geometry Enhancement Module (TGEM), which leverages geometric consistency across successive frames to enhance depth perception and improve scene understanding. Additionally, we present the Temporal Instance-aware Query Generation (TIQG) module, which strategically incorporates temporal cues into the query generation process, enabling a more comprehensive exploration of instance-aware information across frames. Experimental results demonstrate that the proposed GTA-Net outperforms existing monocular 3D lane detection methods.

References

- [1] Florent Alché and Arnaud de La Fortelle. An lstm network for highway trajectory prediction. In *IEEE 20th international conference on intelligent transportation systems*, 2017. 1
- [2] Yifeng Bai, Zhirong Chen, Zhangjie Fu, Lang Peng, Pengpeng Liang, and Erkang Cheng. Curveformer: 3d lane detection by curve propagation with curve queries and attention. In *IEEE International Conference on Robotics and Automation*, 2023. 1, 2, 6, 7
- [3] Yifeng Bai, Zhirong Chen, Pengpeng Liang, and Erkang Cheng. Curveformer++: 3d lane detection by curve propagation with temporal curve queries and attention. *arXiv preprint arXiv:2402.06423*, 2024. 2, 6, 7
- [4] Nicolas Carion, Francisco Massa, Gabriel Synnaeve, Nicolas Usunier, Alexander Kirillov, and Sergey Zagoruyko. End-to-end object detection with transformers. In *European conference on computer vision*, 2020. 2
- [5] Li Chen, Chonghao Sima, Yang Li, Zehan Zheng, Jiajie Xu, Xiangwei Geng, Hongyang Li, Conghui He, Jianping Shi, Yu Qiao, et al. Persformer: 3d lane detection via perspective transformer and the openlane benchmark. In *European Conference on Computer Vision*, 2022. 1, 2, 3, 6, 7
- [6] Ziyi Chen, Kate Smith-Miles, Bo Du, Guoqi Qian, and Mingming Gong. An efficient transformer for simultaneous learning of bev and lane representations in 3d lane detection. *arXiv preprint arXiv:2306.04927*, 2023. 3
- [7] Kun Dong, Jian Xue, Xing Lan, and Ke Lu. 3dlaneformer: Rethinking learning views for 3d lane detection. In *IEEE International Conference on Image Processing*, 2024. 6, 7
- [8] Alexey Dosovitskiy, Lucas Beyer, Alexander Kolesnikov, Dirk Weissenborn, Xiaohua Zhai, Thomas Unterthiner, Mostafa Dehghani, Matthias Minderer, Georg Heigold, Sylvain Gelly, et al. An image is worth 16x16 words: Transformers for image recognition at scale. *arXiv preprint arXiv:2010.11929*, 2020. 2
- [9] Zhengyang Feng, Shaohua Guo, Xin Tan, Ke Xu, Min Wang, and Lizhuang Ma. Rethinking efficient lane detection via curve modeling. In *Proceedings of the IEEE/CVF Conference on Computer Vision and Pattern Recognition*, 2022. 3
- [10] Noa Garnett, Rafi Cohen, Tomer Pe'er, Roei Lahav, and Dan Levi. 3d-lanenet: end-to-end 3d multiple lane detection. In *Proceedings of the IEEE/CVF International Conference on Computer Vision*, 2019. 1, 2, 3, 6, 7
- [11] Xiaodong Gu, Zhiwen Fan, Siyu Zhu, Zuozhuo Dai, Feitong Tan, and Ping Tan. Cascade cost volume for high-resolution multi-view stereo and stereo matching. In *Proceedings of the IEEE/CVF Conference on Computer Vision and Pattern Recognition*, 2020. 4
- [12] Weizhi Guo, Chaochao Li, Kaijiang Li, Pei Lv, and Mingliang Xu. Califree3dlane: Calibration free spatio-temporal bev representation for monocular 3d lane detection. *IEEE Transactions on Intelligent Transportation Systems*, 2024. 6, 7
- [13] Yuliang Guo, Guang Chen, Peitao Zhao, Weide Zhang, Jinghao Miao, Jingao Wang, and Tae Eun Choe. Gen-lanenet: A generalized and scalable approach for 3d lane detection. In *European Conference on Computer Vision*, 2020. 1, 2, 3, 6, 7
- [14] Jianhua Han, Xiajun Deng, Xinyue Cai, Zhen Yang, Hang Xu, Chunjing Xu, and Xiaodan Liang. Laneformer: Object-aware row-column transformers for lane detection. In *Proceedings of the AAAI conference on artificial intelligence*, 2022. 2
- [15] Wencheng Han and Jianbing Shen. Decoupling the curve modeling and pavement regression for lane detection. *arXiv preprint arXiv:2309.10533*, 2023. 6, 7
- [16] Kaiming He, Xiangyu Zhang, Shaoqing Ren, and Jian Sun. Deep residual learning for image recognition. In *Proceedings of the IEEE conference on computer vision and pattern recognition*, 2016. 7
- [17] Shaofei Huang, Zhenwei Shen, Zehao Huang, Zi-han Ding, Jiao Dai, Jizhong Han, Naiyan Wang, and Si Liu. Anchor3dlane: Learning to regress 3d anchors for monocular 3d lane detection. In *Proceedings of the IEEE/CVF Conference on Computer Vision and Pattern Recognition*, 2023. 1, 2, 3, 6, 7
- [18] Shaofei Huang, Zhenwei Shen, Zehao Huang, Yue Liao, Jizhong Han, Naiyan Wang, and Si Liu. Anchor3dlane++: 3d lane detection via sample-adaptive sparse 3d anchor regression. *IEEE Transactions on Pattern Analysis and Machine Intelligence*, 2025. 7
- [19] Dongkwon Jin, Wonhui Park, Seong-Gyun Jeong, Heeyeon Kwon, and Chang-Su Kim. Eigenlanes: Data-driven lane descriptors for structurally diverse lanes. In *Proceedings of the IEEE/CVF Conference on Computer Vision and Pattern Recognition*, 2022. 3
- [20] Dongkwon Jin, Dahyun Kim, and Chang-Su Kim. Recursive video lane detection. In *Proceedings of the IEEE/CVF International Conference on Computer Vision*, 2023. 2
- [21] Alexander Kirillov, Eric Mintun, Nikhila Ravi, Hanzi Mao, Chloe Rolland, Laura Gustafson, Tete Xiao, Spencer Whitehead, Alexander C Berg, Wan-Yen Lo, et al. Segment anything. In *Proceedings of the IEEE/CVF International Conference on Computer Vision*, 2023. 2
- [22] Yeongmin Ko, Younkwan Lee, Shoaib Azam, Farzeen Munir, Moongu Jeon, and Witold Pedrycz. Key points estimation and point instance segmentation approach for lane detection. *IEEE Transactions on Intelligent Transportation Systems*, 2021. 2, 3
- [23] Qi Li, Yue Wang, Yilun Wang, and Hang Zhao. Hdmapnet: An online hd map construction and evaluation framework. In *International Conference on Robotics and Automation*, 2022. 1
- [24] Xuelong Li, Zhiyuan Zhao, and Qi Wang. Absnet: Attention-based spatial segmentation network for traffic scene understanding. *IEEE Transactions on Cybernetics*, 2021. 2
- [25] Zhuoling Li, Chunrui Han, Zheng Ge, Jinrong Yang, En Yu, Haoqian Wang, Hengshuang Zhao, and Xiangyu Zhang. Grouplane: End-to-end 3d lane detection with channel-wise grouping. *arXiv preprint arXiv:2307.09472*, 2023. 3
- [26] Zhuoling Li, Chunrui Han, Zheng Ge, Jinrong Yang, En Yu, Haoqian Wang, Xiangyu Zhang, and Hengshuang Zhao.

- Grouplane: End-to-end 3d lane detection with channel-wise grouping. *IEEE Robotics and Automation Letters*, 2024. 6, 7
- [27] Bencheng Liao, Shaoyu Chen, Xinggang Wang, Tianheng Cheng, Qian Zhang, Wenyu Liu, and Chang Huang. Maptr: Structured modeling and learning for online vectorized hd map construction. *arXiv preprint arXiv:2208.14437*, 2022. 1
- [28] Tsung-Yi Lin, Priya Goyal, Ross Girshick, Kaiming He, and Piotr Dollár. Focal loss for dense object detection. In *Proceedings of the IEEE international conference on computer vision*, 2017. 6
- [29] Lizhe Liu, Xiaohao Chen, Siyu Zhu, and Ping Tan. Condlanenet: a top-to-down lane detection framework based on conditional convolution. In *Proceedings of the IEEE/CVF international conference on computer vision*, 2021. 3
- [30] Ruijin Liu, Zejian Yuan, Tie Liu, and Zhiliang Xiong. End-to-end lane shape prediction with transformers. In *Proceedings of the IEEE/CVF winter conference on applications of computer vision*, 2021. 3
- [31] Ruijin Liu, Dapeng Chen, Tie Liu, Zhiliang Xiong, and Zejian Yuan. Learning to predict 3d lane shape and camera pose from a single image via geometry constraints. In *Proceedings of the AAAI Conference on Artificial Intelligence*, 2022. 2
- [32] Yicheng Liu, Tianyuan Yuan, Yue Wang, Yilun Wang, and Hang Zhao. Vectormapnet: End-to-end vectorized hd map learning. In *International Conference on Machine Learning*, 2023. 1
- [33] Yueru Luo, Xu Yan, Chaoda Zheng, Chao Zheng, Shuqi Mei, Tang Kun, Shuguang Cui, and Zhen Li M^{*}. M²-3dlanenet: Multi-modal 3d lane detection. *arXiv preprint arXiv:2209.05996*, 2022. 3
- [34] Yueru Luo, Shuguang Cui, and Zhen Li. Dv-3dlane: End-to-end multi-modal 3d lane detection with dual-view representation. In *International Conference on Learning Representations*, 2023. 3
- [35] Yueru Luo, Chaoda Zheng, Xu Yan, Tang Kun, Chao Zheng, Shuguang Cui, and Zhen Li. Latr: 3d lane detection from monocular images with transformer. In *Proceedings of the IEEE/CVF International Conference on Computer Vision*, 2023. 2, 3, 7
- [36] Fulong Ma, Weiqing Qi, Guoyang Zhao, Linwei Zheng, Sheng Wang, and Ming Liu. Monocular 3d lane detection for autonomous driving: Recent achievements, challenges, and outlooks. *arXiv preprint arXiv:2404.06860*, 2024. 1, 3
- [37] Anuar Mikdad Muad, Aini Hussain, S Abdul Samad, Mohd Marzuki Mustaffa, and BURHANUDDIN YEOP Majlis. Implementation of inverse perspective mapping algorithm for the development of an automatic lane tracking system. In *IEEE Region 10 Conference TENCON.*, 2004. 2
- [38] Maximilian Pittner, Joel Janai, and Alexandru P Condurache. Lanecpp: Continuous 3d lane detection using physical priors. In *Proceedings of the IEEE/CVF Conference on Computer Vision and Pattern Recognition*, 2024. 7
- [39] Zequn Qin, Huanyu Wang, and Xi Li. Ultra fast structure-aware deep lane detection. In *European Conference on Computer Vision*, 2020. 3
- [40] Zequn Qin, Pengyi Zhang, and Xi Li. Ultra fast deep lane detection with hybrid anchor driven ordinal classification. *IEEE Transactions on Pattern Analysis and Machine Intelligence*, 2022. 2, 3
- [41] Zhan Qu, Huan Jin, Yang Zhou, Zhen Yang, and Wei Zhang. Focus on local: Detecting lane marker from bottom up via key point. In *Proceedings of the IEEE/CVF Conference on Computer Vision and Pattern Recognition*, 2021. 3
- [42] Pei Sun, Henrik Kretzschmar, Xerxes Dotiwalla, Aurelien Chouard, Vijaysai Patnaik, Paul Tsui, James Guo, Yin Zhou, Yuning Chai, Benjamin Caine, et al. Scalability in perception for autonomous driving: Waymo open dataset. In *Proceedings of the IEEE/CVF Conference on Computer Vision and Pattern Recognition*, 2020. 7
- [43] Lucas Tabelini, Rodrigo Berriel, Thiago M Paixao, Claudine Badue, Alberto F De Souza, and Thiago Oliveira-Santos. Keep your eyes on the lane: Real-time attention-guided lane detection. In *Proceedings of the IEEE/CVF Conference on Computer Vision and Pattern Recognition*, 2021. 3
- [44] Lucas Tabelini, Rodrigo Berriel, Thiago M Paixao, Claudine Badue, Alberto F De Souza, and Thiago Oliveira-Santos. Polylanenet: Lane estimation via deep polynomial regression. In *International Conference on Pattern Recognition*, 2021. 3
- [45] Jigang Tang, Songbin Li, and Peng Liu. A review of lane detection methods based on deep learning. *Pattern Recognition*, 2021. 2
- [46] Jin Wang, Stefan Schroedl, Klaus Mezger, Roland Ortloff, Armin Joos, and Thomas Passegger. Lane keeping based on location technology. *IEEE Transactions on Intelligent Transportation Systems*, 2005. 1
- [47] Jinsheng Wang, Yinchao Ma, Shaofei Huang, Tianrui Hui, Fei Wang, Chen Qian, and Tianzhu Zhang. A keypoint-based global association network for lane detection. In *Proceedings of the IEEE/CVF Conference on Computer Vision and Pattern Recognition*, 2022. 2, 3
- [48] Ruihao Wang, Jian Qin, Kaiying Li, Yaochen Li, Dong Cao, and Jintao Xu. Bev-lanedet: a simple and effective 3d lane detection baseline. In *Proceedings of the IEEE/CVF Conference on Computer Vision and Pattern Recognition*, 2023. 2, 6, 7
- [49] Jamie Watson, Oisín Mac Aodha, Victor Prisacariu, Gabriel Brostow, and Michael Firman. The temporal opportunist: Self-supervised multi-frame monocular depth. In *Proceedings of the IEEE/CVF Conference on Computer Vision and Pattern Recognition*, 2021. 4
- [50] Kyle R Williams, Rachel Schlossman, Daniel Whitten, Joe Ingram, Srideep Musuvathy, James Pagan, Kyle A Williams, Sam Green, Anirudh Patel, Anirban Mazumdar, et al. Trajectory planning with deep reinforcement learning in high-level action spaces. *IEEE Transactions on Aerospace and Electronic Systems*, 2022. 1
- [51] Dongming Wu, Jiahao Chang, Fan Jia, Yingfei Liu, Tiancai Wang, and Jianbing Shen. Topomlp: An simple yet strong pipeline for driving topology reasoning. *arXiv preprint arXiv:2310.06753*, 2023. 2
- [52] Zhuofan Xia, Xuran Pan, Shiji Song, Li Erran Li, and Gao Huang. Vision transformer with deformable attention. In

Proceedings of the IEEE/CVF Conference on Computer Vision and Pattern Recognition, 2022. 4

- [53] Hang Xu, Shaoju Wang, Xinyue Cai, Wei Zhang, Xiaodan Liang, and Zhenguo Li. Curvelane-nas: Unifying lane-sensitive architecture search and adaptive point blending. In *Computer Vision–ECCV 2020: 16th European Conference, Glasgow, UK, August 23–28, 2020, Proceedings, Part XV 16*, 2020. 2
- [54] Fan Yan, Ming Nie, Xinyue Cai, Jianhua Han, Hang Xu, Zhen Yang, Chaoqiang Ye, Yanwei Fu, Michael Bi Mi, and Li Zhang. Once-3dlanes: Building monocular 3d lane detection. In *Proceedings of the IEEE/CVF Conference on Computer Vision and Pattern Recognition*, 2022. 1, 3
- [55] Jiayu Yang, Wei Mao, Jose M Alvarez, and Miaomiao Liu. Cost volume pyramid based depth inference for multi-view stereo. In *Proceedings of the IEEE/CVF Conference on Computer Vision and Pattern Recognition*, 2020. 4
- [56] Seungwoo Yoo, Hee Seok Lee, Heesoo Myeong, Sungrack Yun, Hyoungwoo Park, Janghoon Cho, and Duck Hoon Kim. End-to-end lane marker detection via row-wise classification. In *Proceedings of the IEEE/CVF Conference on Computer Vision and Pattern Recognition workshops*, 2020. 3
- [57] Runkai Zhao, Heng Wang, and Weidong Cai. Lanecmkt: Boosting monocular 3d lane detection with cross-modal knowledge transfer. In *Proceedings of the 32nd ACM International Conference on Multimedia*, 2024. 6, 7
- [58] Tu Zheng, Hao Fang, Yi Zhang, Wenjian Tang, Zheng Yang, Haifeng Liu, and Deng Cai. Resa: Recurrent feature-shift aggregator for lane detection. In *Proceedings of the AAAI Conference on Artificial Intelligence*, 2021. 2
- [59] Tu Zheng, Yifei Huang, Yang Liu, Wenjian Tang, Zheng Yang, Deng Cai, and Xiaofei He. Clrnet: Cross layer refinement network for lane detection. In *Proceedings of the IEEE/CVF Conference on Computer Vision and Pattern Recognition*, 2022. 2
- [60] Zewen Zheng, Xuemin Zhang, Yongqiang Mou, Xiang Gao, Chengxin Li, Guoheng Huang, Chi-Man Pun, and Xiaochen Yuan. Pvalane: Prior-guided 3d lane detection with view-agnostic feature alignment. In *Proceedings of the AAAI Conference on Artificial Intelligence*, 2024. 3
- [61] Xizhou Zhu, Weijie Su, Lewei Lu, Bin Li, Xiaogang Wang, and Jifeng Dai. Deformable detr: Deformable transformers for end-to-end object detection. *arXiv preprint arXiv:2010.04159*, 2020. 4